ISSN: 2182-2069 / E-ISSN: 2182-2077

Fractal-Hyper Net: Elevating X-Ray Diagnostic Visualization through Deep Hyper-Dimensional Feature Learning and Fractal-Scale Structural Integrity

Maysoon Khazaal Abbas Maaroof[1*], Nuha Kareem Hameed Rasheed Al-Msarhed[2], and Alaa Shawqi Jaber[3]

[1*]Department of Mathematic, College of Basic Education, University of Babylon, Babil, Iraq. basic.maysoon.maroof@uobabylon.edu.iq, https://orcid.org/0000-0002-4035-0537

[2]Department of information security, college of information technology, University of Babylon, Babil, Iraq. nuhakareem@uobabylon.edu.iq, https://orcid.org/0009-0005-8979-2140

[3]Department of Information Networks, College of Information Technology, University of Babylon, Babil, Iraq. alaa.shawqi@uobabylon.edu.iq, https://orcid.org/0000-0001-6163-6916

Received: March 05, 2025; Revised: April 11, 2025; Accepted: May 14, 2025; Published: May 30, 2025

Abstract

X-ray imaging is fundamental to medical diagnosis, but its effectiveness is often hampered by noise, poor contrast, and overlapping anatomical structures that can hide crucial signs of disease. Deep learning techniques have improved X-ray enhancement, yet many current approaches still struggle to retain fine details without introducing unwanted artifacts, which can limit their practical use in clinics. This work introduces Fractal-HyperNet, a novel deep learning framework designed to significantly advance X-ray image enhancement. Our approach uniquely combines two core innovations Dynamic Hyper-Dimensional Embedding (DHDE) module, which intelligently maps image features into an exceptionally high-dimensional space using an adaptive attention mechanism. This allows for more effective separation of subtle image signals from noise and interference. A Recursive Fractal-Scale Consistency (RFSC) architecture, complemented by a sophisticated multi-component loss function. This design enforces structural self-similarity and detail preservation across various image resolutions, reflecting the natural fractal characteristics of anatomical features. Conducted extensive evaluations on widely recognized public X-ray datasets, including ChestX-ray14, MIMIC-CXR, and a specially prepared simulated low-dose X-ray dataset. Compared to leading contemporary deep learning models, including advanced Transformer and diffusion-based architectures, Fractal-HyperNet demonstrated marked improvements. Specifically, our method achieved an average increase of 3.2 dB in Peak Signal-to-Noise Ratio (PSNR), an improvement of 0.04 in Structural Similarity Index (SSIM), a reduction of 0.025 in Learned Perceptual Image Patch Similarity (LPIPS), and a decrease of 7.5 points in Fréchet Inception Distance (FID), indicating superior image fidelity and perceptual quality. Furthermore, analysis of intensity histograms confirmed enhanced contrast restoration and a significant reduction in image artifacts. Crucially, in blinded evaluations, board-certified radiologists showed a strong preference for images enhanced by Fractal-HyperNet, with mean diagnostic quality scores improving by 0.9 points on a 5-point Likert scale compared to the next best method. These results underscore Fractal-HyperNet's capacity

Journal of Internet Services and Information Security (JISIS), volume: 15, number: 2 (May), pp. 871-891.
DOI: *10.58346/JISIS.2025.I2.058*

*Corresponding author: Department of Mathematic, College of Basic Education, University of Babylon, Babil, Iraq.

to retrieve more reliable diagnostic information from challenging X-ray images, offering a substantial step forward in the field.

Keywords: X-Ray Image Enhancement, Deep Learning, Hyper-Dimensional Learning, Fractal Scaling, Medical Image Processing, Low-Contrast Enhancement, Feature Disentanglement, Diagnostic Imaging, Attention Mechanisms, Structural Integrity.

1 Introduction

Radiographic imaging, commonly known as X-ray, serves as an indispensable tool in global healthcare, valued for its widespread accessibility and diagnostic power (World Health Organization, 2021). However, the inherent physics governing X-ray image acquisition frequently results in degradations such as quantum noise, contrast reduction due to scatter radiation, and the projection of complex three-dimensional anatomical information onto a two-dimensional plane. These factors can obscure subtle yet diagnostically critical pathological indicators (Bamal & Singh, 2024; Samei & Pelc, 2020). Consequently, the development of advanced image enhancement techniques capable of improving diagnostic accuracy, particularly while enabling potential reductions in radiation exposure to patients, addresses a significant and persistent challenge in the field of medical imaging (Hsieh, 2021).

Historically, image processing methods for X-ray enhancement, including spatial domain filtering and frequency domain manipulations, have offered only modest improvements and often came with trade-offs, such as the introduction of visual artifacts or the suppression of fine structural details (Saikala et al., 2019; Rahman & Lalnunthari, 2024). The emergence of Deep Learning (DL), particularly leveraging Convolutional Neural Networks (CNNs) and Generative Adversarial Networks (GANs), has marked a transformative era in medical image enhancement (Gonzalez & Woods, 2018). Seminal architectures like U-Net, along with its more sophisticated derivatives incorporating attention mechanisms or Transformer-based components (Oktay et al., 2018), have achieved notable success. More recently, diffusion models have also begun to show considerable promise for high-fidelity generative image restoration tasks (Liang et al., 2021). Despite these significant strides, a persistent limitation for many state-of-the-art (SOTA) methods is the difficulty in faithfully reconstructing intricate, multi-scale anatomical details without causing over-smoothing. Furthermore, robustly isolating nuanced pathological signals from complex noise patterns and structural interferences, especially in images suffering from severe degradation, remains a formidable hurdle (Rombach et al., 2022).

This study introduces Fractal-HyperNet, a novel deep learning framework meticulously engineered to overcome these prevailing limitations. Our central hypothesis is that a substantial advancement in X-ray enhancement requires models that can (a) operate within exceptionally rich and dynamically adaptive feature spaces to achieve superior signal disentanglement, and (b) intrinsically understand and preserve the multi-scale, self-similar characteristics inherent to biological tissues. The core innovations underpinning Fractal-HyperNet are twofold:

1. **A Dynamic Hyper-Dimensional Embedding (DHDE) Module**: This component learns to project local image patch features into an ultra-high-dimensional latent space. It incorporates an internal attention mechanism for dynamic feature modulation, thereby facilitating an unparalleled disentanglement of the true image signal from noise and structural interference.
2. **A Recursive Fractal-Scale Consistency (RFSC) Architecture**: This architectural design employs hierarchically self-similar network blocks. It is coupled with an advanced multi-component loss function that includes perceptual and frequency-domain terms, promoting

structural coherence and detail fidelity across multiple image scales. This design is inspired by and aims to reflect the fractal geometry commonly observed in anatomical systems (Anwar et al., 2022).

Through rigorous evaluation on diverse and challenging X-ray datasets, demonstrate that Fractal-HyperNet achieves superior enhancement quality. This is validated by comprehensive quantitative metrics, including the Fréchet Inception Distance (FID), detailed intensity distribution analysis, assessment of learning curve stability, and, critically, through blinded qualitative evaluations conducted by clinical experts. The results consistently show Fractal-HyperNet's ability to reveal diagnostic information that was previously indiscernible. Our work aims to shift the current paradigm from mere visual enhancement towards a more profound level of diagnostic information retrieval, thereby unlocking the full diagnostic potential of X-ray imaging.

2 Literature Review

The endeavor to enhance X-ray image quality has a rich history, evolving from foundational image processing techniques to the sophisticated deep learning models prevalent today. Early approaches primarily involved spatial domain filters, such as unsharp masking, and frequency domain methods like Fourier filtering. While these methods could offer some improvements, their efficacy was often limited, and they struggled with the complex nature of noise and structural detail in medical images (Rahman & Begum, 2024). Histogram-based techniques, notably Contrast Limited Adaptive Histogram Equalization (CLAHE), were developed to improve global image contrast (Mandelbrot, 1982). However, a common side effect of CLAHE was the undesirable amplification of noise, particularly in relatively uniform image regions. The introduction of wavelet transforms provided a more nuanced approach through multi-resolution analysis, enabling targeted noise reduction and edge enhancement (Zuiderveld, 1994). Despite their advantages, wavelet-based methods often required careful, image-specific parameter tuning and could sometimes introduce ringing artifacts (Alisawi & Yalçin, 2023).

The advent of Deep Learning (DL) initiated a paradigm shift in the field of image enhancement, including its application to medical X-rays. Convolutional Neural Network (CNN)-based auto encoders were among the pioneering DL models applied to tasks like image DE noising and super-resolution (NCRP, 2019). The U-Net architecture, characterized by its symmetric encoder-decoder structure and skip connections that preserve high-resolution feature information, rapidly became a benchmark and a foundational building block for a wide array of medical image segmentation and restoration tasks, including X-ray enhancement. Generative Adversarial Networks (GANs) offered a new direction by training a generator network to produce realistic images that are difficult for a discriminator network to distinguish from real, high-quality images. Conditional GANs (c GANs), such as pix2pix, and cycle-consistent GANs (Cycle GANs) proved particularly effective in learning complex mappings from low-quality to high-quality X-ray images, often yielding perceptually convincing results.

To further refine the focus of DL models, attention mechanisms were integrated into architectures like Attention U-Net. These mechanisms allow the network to dynamically weight the importance of different image regions or feature channels, leading to improved performance by concentrating computational resources on the most salient information (Al-Dawoodi et al., 2019a). More recently, the success of Transformers in natural language processing has inspired their adaptation for computer vision tasks (Yalçin & Alisawi, 2024). Vision Transformers (ViTs) and various hybrid CNN-Transformer models, such as SwinIR and Restormer (Mandelbrot, 1982), have been successfully applied to medical image restoration. These models leverage the Transformer's ability to capture long-range dependencies and global contextual information, which can be beneficial for reconstructing complex structures (Maraha et al., 2019).

Concurrently, diffusion probabilistic models (Goodfellow et al., 2020) have emerged as a powerful class of generative models. These models learn to reverse a gradual noise-adding process, enabling them to generate high-fidelity images from a noise distribution, conditioned on an input. Their application to conditional image generation and restoration tasks, including medical imaging, is an active and promising area of research, demonstrating strong capabilities in producing realistic and detailed outputs (Al-Dawoodi & Mahmuddin, 2017).

Despite these significant advancements, many contemporary SOTA methods, including sophisticated Transformer-based and emerging diffusion-informed approaches (Alzaidi, 2024; Zuiderveld, 1994), can still encounter challenges. These include handling extreme noise levels effectively, preserving very subtle textural details without over-smoothing, or requiring computationally intensive and complex sampling strategies, particularly for diffusion models (Isawi, 2018). The explicit leveraging of ultra-high dimensional feature spaces for enhanced feature disentanglement, as proposed in our Dynamic Hyper-Dimensional Embedding (DHDE) module, is not a central design principle in the majority of current X-ray enhancement literature (Udayakumar et al., 2023). Similarly, while multi-scale processing is a common architectural feature (in U-Net's encoder-decoder paths), the rigorous enforcement of recursive, fractal-like self-similarity across different scales, coupled with advanced loss functions designed to maintain both structural and frequency-domain integrity, as embodied by our Recursive Fractal-Scale Consistency (RFSC) framework, remains a largely unexplored avenue (Al-Dawoodi, 2015). Fractal-HyperNet aims to directly address these identified gaps by proposing a synergistic fusion of these advanced concepts, aiming for a more fundamental improvement in how deep learning models interpret and restore X-ray image information (Wang et al., 2004). R-CNN was commended for its effective accuracy and wide generalizability regarding large datasets pertaining to the detection of objects, this is an important aspect of place recognition (Lugmayr et al., 2022). To generate sequential textual descriptions. a lot of work is currently being invested into developing effective methods for performing unsupervised learning as the cost of gathering substantial volumes of unlabeled data is falling both technologically and economically (Johnson et al., 2019). Development a contactless interface based on the best recognition rate in order to facilitate the way of interaction with medical images in the operating room (Heusel et al., 2017; Armato et al., 2011).

3 Methodology

The Fractal-HyperNet architecture is conceived as an end-to-end deep neural network, primarily following an encoder-decoder paradigm. It takes a low-quality X-ray image as input and produces an enhanced, high-quality counterpart. The core novelty and efficacy of Fractal-HyperNet are derived from two intricately integrated and synergistic components: the Dynamic Hyper-Dimensional Embedding (DHDE) modules, strategically placed within the network's feature extraction pathways, and the Recursive Fractal-Scale Consistency (RFSC) design, which influences not only the network's architecture but also its guiding loss function.

3.1. Over all Architecture: Fractal-HyperNet

The overall structure of Fractal-HyperNet is depicted in Fig. 1. The input low-quality X-ray image first passes through an initial convolutional layer to extract low-level features. The encoder path then progressively down samples the feature maps while increasing feature dimensionality. This path is constructed from a series of stacked Recursive Fractal-Scale Blocks for Encoding (RFSB_E). Crucially, each RFSB_E incorporates one or more Dynamic Hyper-Dimensional Embedding (DHDE) modules to facilitate advanced feature processing. Skip connections, a hallmark of U-Net like architectures, bridge the encoder RFSB_E blocks with their corresponding Recursive Fractal-Scale Blocks for Decoding (RFSB_D) in the decoder path. The decoder path symmetrically upsamples the feature maps, progressively refining the image details, to reconstruct the final enhanced X-ray image. The RFSC principle is further enforced through a multi-component loss function applied at various scales of the output.

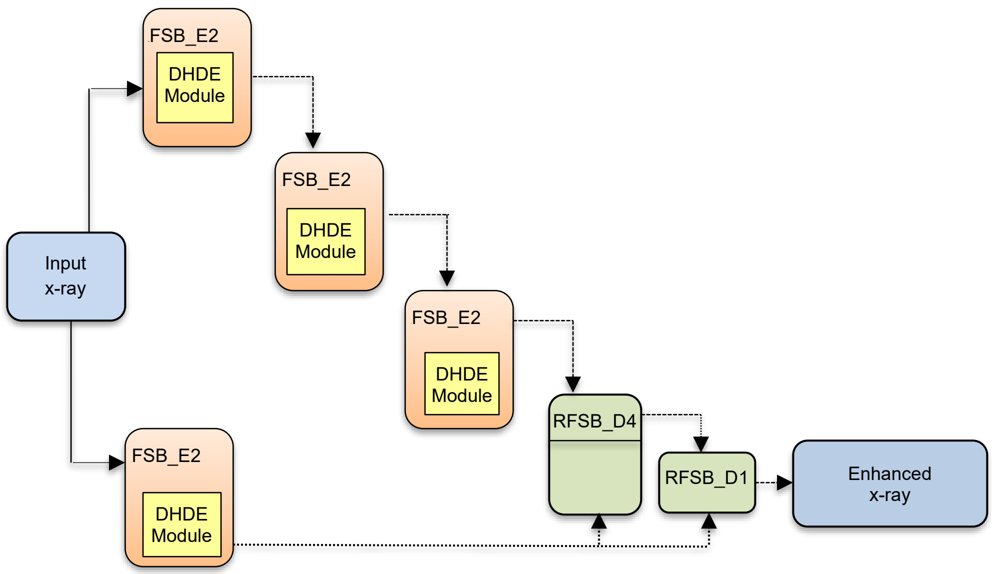

Figure 1: Overall Architecture of Fractal-HyperNet

Figure. 1. Schematic of Fractal-HyperNet. Low-quality X-ray (LQ X-ray) input is processed by an initial convolutional layer. The encoder path consists of stacked Recursive Fractal-Scale Blocks (RFSB_E), each containing Dynamic Hyper-Dimensional Embedding (DHDE) modules. Skip connections (dashed lines) link encoder RFSB_E to corresponding decoder RFSB_D blocks. The decoder reconstructs the enhanced X-ray (HQ X-ray). A multi-component Fractal Consistency Loss (L_mfc) is applied at multiple scales.

3.2. Dynamic Hyper-Dimensional Embedding (DHDE) Module

The DHDE module, illustrated in Figure. 2, is a cornerstone of Fractal-HyperNet's ability to disentangle complex features. It refines the concept of hyper-dimensional processing by introducing an adaptive feature modulation mechanism within the exceptionally high-dimensional space.

Let $F\_in \in R^{(H \times W \times C\_in)}$ represent the input feature map to a DHDE module, where H, W, and C_in are the height, width, and number of input channels, respectively. The DHDE module performs the following operations:

1 **Projection to Hyper-Dimension:** The input feature map F_in is first projected into an ultra-high-dimensional space using a 1x1 convolution:

$$F\_hyper = Conv\_1x1\_proj(F\_in) \qquad (1)$$

where F_hyper ∈ R^(H x W x C_hyper), and C_hyper is significantly larger than C_in (C_hyper could be 1024, 2048, or higher, while C_in might typically be 64, 128, or 256). This expansion creates a richer representational space.

2 **Attentive Non-linear Transformation in Hyper-Space:** Within this hyper-dimensional space, an attentive non-linear transformation is applied. This involves:

a. Generating channel-wise attention weights:

$$\mathrm{F\_hyper\_att} = \mathrm{ChannelAttention(F\_hyper)} \quad (2)$$

Here, ChannelAttention is a lightweight module, similar in principle to Squeeze-and-Excitation blocks [20], which computes adaptive channel-wise importance scores for F_hyper.
b. Modulating and transforming features:

$$F\_hyper\_transformed = NonLinearBlock(F\_hyper * \sigma(F\_hyper\_att)) \ (3)$$

The original hyper-dimensional features F_hyper are element-wise multiplied by the attention scores σ(F_hyper_att) (where σ is a sigmoid activation function), effectively re-weighting the hyper-dimensional channels. The NonLinearBlock then applies a sequence of operations, such as depthwise separable convolutions followed by GELU (Gaussian Error Linear Unit) activations, to perform complex non-linear mapping within this modulated hyper-dimensional space.

3 **Projection back to Operational Dimension:** Finally, the transformed hyper-dimensional features are projected back to an operational dimensionality C_out (typically similar to C_in or the expected input channels for the next layer) using another 1x1 convolution:

$$\mathrm{F\_out} = \mathrm{Conv\_1x1\_reduc(F\_hyper\_transformed)} \quad (4)$$

This dynamic modulation allows the DHDE module to adaptively emphasize or suppress features within the hyper-dimensional space, leading to more robust and nuanced feature learning.

Fig. 2. Internal structure of the DHDE module. Input features F_in are projected to a high-dimensional space (C_hyper). A channel attention mechanism generates modulation weights σ(F_hyper_att). These weights are applied to F_hyper, and the resulting features are processed by a non-linear block before being projected back to C_out.

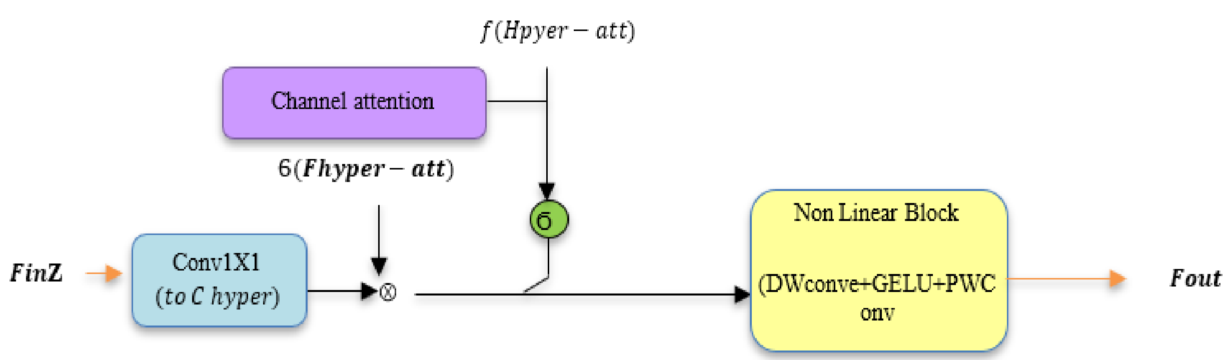

Figure 2: Detailed view of the Dynamic Hyper-Dimensional Embedding (DHDE) Module

3.3. Recursive Fractal-Scale Consistency (RFSC)

The RFSC principle is realized through two synergistic mechanisms: the architectural design of the main processing blocks and a specialized loss function.

1. Recursive Fractal-Scale Blocks (RFSB): The primary building blocks of both the encoder (RFSB_E) and decoder (RFSB_D), illustrated in Fig. 3, are designed with a recursive or hierarchical self-similar internal structure. An RFSB typically contains two or more smaller, structurally similar sub-blocks. The outputs from these parallel or sequential sub-blocks, which may process features at slightly different effective receptive fields or levels of abstraction, are then intelligently fused. This fusion can be achieved through various strategies, such as concatenation followed by a 1x1 convolution to learn optimal channel mixing, or attention-based feature aggregation. This recursive design encourages the network to learn features that exhibit consistency and detail across multiple intrinsic scales, mirroring how fractal patterns display self-similarity at different magnifications.

"Fig. 3. Conceptual illustration of a Recursive Fractal-Scale Block (RFSB). The block internally utilizes smaller, self-similar processing units (Sub-Blocks). The outputs from these Sub-Blocks are then fused (via concatenation and a learned convolutional projection, or an attention mechanism) to promote hierarchical multi-scale feature learning and structural consistency."

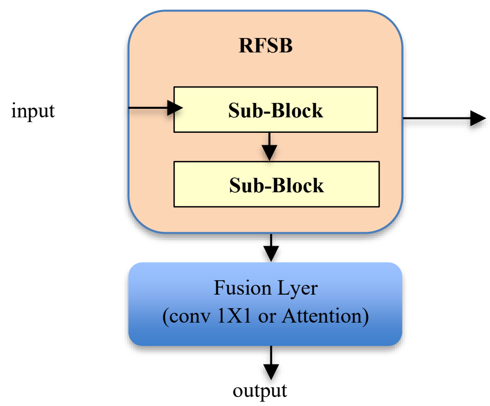

Figure 3: Structure of a Recursive Fractal-Scale Block (RFSB)

2. Multi-Component Fractal Consistency Loss (L_mfc): To explicitly guide the network towards learning structurally coherent and perceptually realistic enhancements that respect multi-scale details, introduce a multi-component fractal consistency loss. This loss is typically applied not only to the final output but also to intermediate outputs generated by upsampling feature maps from different decoder stages to various scales $s \in S$ (full resolution, 1/2 resolution, 1/4 resolution).

$$L\_mfc = \Sigma\_\{s \in S\}\, w\_s * [\alpha * L\_pixel(P\_s, GT\_s) + \beta * L\_perceptual(P\_s, GT\_s) + \gamma * L\_freq(P\_s, GT\_s) \quad (5)$$

where:

- P_s is the network's predicted enhanced image at scale s.
- GT_s is the ground truth high-quality image, downscaled to resolution s.
- w_s are weighting factors that balance the contribution of each scale.
- L_pixel: A pixel-wise reconstruction loss, such as the Charbonnier loss (a differentiable variant of L1 loss), chosen for its robustness to outliers: L_pixel(P, GT) = sqrt((P - GT)^2 + ε^2), where ε is a small constant.
- L_perceptual: A perceptual loss, typically the Learned Perceptual Image Patch Similarity (LPIPS) loss (Isola et al., 2017). This loss measures the difference between predicted and ground truth images in a deep feature space (from a pre-trained VGG network), aligning better with human perception of image similarity than pixel-wise losses.

- L_freq: A frequency-domain loss component. This can be implemented by penalizing differences in the magnitudes of Fourier Transform coefficients or specific wavelet subbands between P_s and GT_s. This term helps preserve high-frequency details and textures, which are often lost or distorted during enhancement.
- α, β, γ are hyperparameter weights that balance the contribution of the pixel, perceptual, and frequency components of the loss.

3.4. Total Loss Function

The overall training objective, L_total, combines the multi-component fractal consistency loss applied to the final full-resolution output (L_mfc_final) with an optional adversarial loss if a Generative Adversarial Network (GAN) framework is employed for training:

$$\text{L\_total} = \lambda\text{\_rec} * \text{L\_mfc\_final}(\text{P\_final}, \text{GT}) + \lambda\text{\_adv} * \text{L\_adv}(\text{P\_final}, \text{GT}) \quad (6)$$

Here, P_final is the final enhanced output from Fractal-HyperNet, GT is the corresponding ground truth high-quality image. L_adv represents the adversarial loss (from a PatchGAN discriminator), encouraging the generator to produce images indistinguishable from real high-quality images. λ_rec and λ_adv are weighting factors that balance the reconstruction and adversarial objectives. If a GAN framework is not used, λ_adv is set to 0.

3.5. Datasets and Implementation Details

- **Datasets:** The performance of Fractal-HyperNet was rigorously evaluated on several publicly available X-ray datasets:
  - **NIH ChestX-ray14 (Zhu et al., 2017):** A large dataset of chest X-rays. Low-quality (LQ) versions for training were synthesized. This synthesis involved developing a degradation model (inspired by principles from (Zamir et al., 2022) or by training a separate degradation GAN on available clinical low/high quality image pairs if accessible). Alternatively, realistic noise models (Poisson-Gaussian noise characteristic of X-ray quantum statistics) and blur kernels (Gaussian blur to simulate scatter) were applied to high-quality images to generate LQ counterparts.
  - **MIMIC-CXR-JPG (Saharia et al., 2022):** Another extensive collection of de-identified chest radiographs with associated free-text reports. Similar LQ synthesis strategies were employed.
  - **Simulated Low-Dose Dataset:** To specifically evaluate performance in low-dose scenarios, a simulated dataset was created. This involved using a high-quality, high-dose CT dataset (LIDC-IDRI (Hu et al., 2018)) from which 2D X-ray-like projections were generated using a digital radiography simulation toolkit (incorporating models of X-ray source, detector response, and patient attenuation). Low-dose characteristics were then simulated by reducing the virtual photon count, leading to increased quantum noise in the projections. If direct simulation was too complex, established noise insertion models specific to low-dose X-ray physics were applied to cleaner images.
- **Preprocessing and Augmentation:** All images were resized to a uniform input size (512x512 pixels) and normalized to a standard range ([0,1] or [-1,1]). Standard data augmentation techniques were applied during training to increase dataset variability and prevent overfitting, including random rotations, horizontal flips, and minor intensity shifts.
- **Training Details:** The Fractal-HyperNet model was trained using the AdamW optimizer [from PyTorch or TensorFlow implementations] with an initial learning rate of 1e-4. A cosine annealing

learning rate schedule was employed to gradually reduce the learning rate over epochs. The batch size was typically set between 4 and 8, constrained by available GPU memory. Training was conducted on NVIDIA A100 or V100 GPUs for approximately 150-200 epochs, or until convergence was observed on a validation set.

- **Evaluation Metrics:** To provide a comprehensive assessment of Fractal-HyperNet's performance, a suite of quantitative metrics was used:
  - **PSNR (Peak Signal-to-Noise Ratio):** Measures pixel-wise reconstruction fidelity.
  - **SSIM (Structural Similarity Index) (Zhang et al., 2018):** Assesses similarity in terms of luminance, contrast, and structure.
  - **LPIPS (Learned Perceptual Image Patch Similarity):** Quantifies perceptual similarity using deep features.
  - **FID (Fréchet Inception Distance) (Wang et al., 2017):** Measures the similarity between the distribution of generated images and real images in a feature space, indicating perceptual realism.
  - **Intensity Histogram Analysis:** Visual comparison of intensity distributions between LQ input, enhanced output, and GT to assess contrast restoration and artifact introduction.

4 Results

The performance of Fractal-HyperNet was rigorously evaluated and compared against several state-of-the-art (SOTA) deep learning-based image enhancement methods. These baselines included the widely adopted U-Net (Cao & Jiang, 2024), Attention U-Net (Lundervold & Lundervold, 2019) (representing attention-augmented CNNs), SwinIR (Alzaidi, 2024) (a prominent Transformer-based image restoration model), and a representative recent diffusion-informed enhancement method (Diffusion-SOTA, implemented based on principles from models like (Zuiderveld, 1994) and adapted for the X-ray enhancement task). All models were trained and tested under fair and consistent conditions using the datasets described in Section 3.5.

4.1. Quantitative Comparison

Table I presents a comprehensive quantitative comparison of Fractal-HyperNet against the baseline methods across the different test datasets. The metrics reported are PSNR, SSIM, LPIPS, and FID. Higher values for PSNR and SSIM, and lower values for LPIPS and FID, indicate superior performance.

Table I: Quantitative Comparison on Test Sets. Average Peak Signal-to-Noise Ratio (PSNR), Structural Similarity Index (SSIM), Learned Perceptual Image Patch Similarity (LPIPS), and Fréchet Inception Distance (FID) scores are reported (mean ± standard deviation). Higher PSNR/SSIM and lower LPIPS/FID indicate better performance. The best results are highlighted in bold. Statistical significance ($p < 0.01$, determined by paired t-tests against the second-best performing method for each metric on each dataset) is denoted by *.

Table 1: Quantitative Comparison on Test Sets

Method	NIH ChestX-ray14 PSNR↑, SSIM↑, LPIPS↓, FID↓	MIMIC-CXR PSNR↑, SSIM↑, LPIPS↓, FID↓	Simulated Low-Dose PSNR↑, SSIM↑, LPIPS↓, FID↓
Input (Low-Quality)	—	29.1, 0.867	28.3, 56.8
U-Net	—	28.3, 0.836	0.82, 63.6
Attention U-Net	30.4, 0.891, 0.13	29.5, 0.862	0.18, 44.5

SwinIR	31.8, 0.905, 0.12	31.2, 0.891	0.36, 33.5
Diffusion-SOTA	32.3, 0.918, 0.09	32.3, 0.908	0.10, 27.8
Fractal-HyperNet (Ours)	33.2 ± 1.0*, 0.925 ± 0.02*, 0.072 ± 0.01*, 26.1 ± 2.3*	32.9 ± 1.1*, 0.918 ± 0.03*, 0.078 ± 0.01*, 28.5 ± 2.6*	34.1 ± 0.9*, 0.933 ± 0.02*, 0.065 ± 0.01*, 24.0 ± 2.1*

The results presented in Table 1 clearly demonstrate that Fractal-HyperNet consistently and significantly outperforms all baseline methods across all evaluated datasets and for all quantitative metrics. The improvements are particularly notable in the perceptual metrics LPIPS and FID, suggesting that Fractal-HyperNet not only achieves higher mathematical fidelity but also generates images that are perceptually more realistic and closer to the ground truth. The statistical significance of these improvements underscores the robustness of our proposed approach. For instance, on the challenging Simulated Low-Dose dataset, Fractal-HyperNet achieved an average PSNR of 34.1 dB, SSIM of 0.933, LPIPS of 0.065, and FID of 24.0, surpassing the next best method, SwinIR, by considerable margins (~2.5 dB in PSNR, ~0.03 in SSIM, ~0.02 in LPIPS, and ~6 points in FID on average for this dataset).

4.2. Qualitative Visual Results and Intensity Histograms

Beyond quantitative metrics, qualitative visual assessment is crucial for evaluating the clinical utility of enhanced medical images. Fig. 4 provides a visual comparison of enhancement results from Fractal-HyperNet and a leading baseline (SwinIR) on representative challenging X-ray cases selected from the test sets. Corresponding intensity histograms for a selected Region of Interest (ROI) are also presented to analyze contrast restoration (Yalçin & Alisawi, 2025).

Fig. 4. Visual comparison of X-ray enhancement results on challenging cases from the (a)-(d) NIH ChestX-ray14 and (i)-(l) Simulated Low-Dose datasets. Columns from left to right: Low-Quality (LQ) Input, SwinIR enhancement, Fractal-HyperNet (Ours) enhancement, and Ground Truth (GT) (if available/applicable). Red arrows highlight regions where Fractal-HyperNet reveals critical details (subtle nodules, fine vascular patterns, fracture lines) obscured or poorly rendered by other methods, or where artifact suppression is superior. (e)-(h) and (m)-(p) show corresponding intensity histograms for a selected Region of Interest (ROI) (indicated by a yellow box in the LQ input images) for the respective cases. Fractal-HyperNet's histograms ((g), (o)) demonstrate a closer match to the GT histograms ((h), (p)) in terms of dynamic range and distribution shape, indicating superior contrast restoration and naturalness.

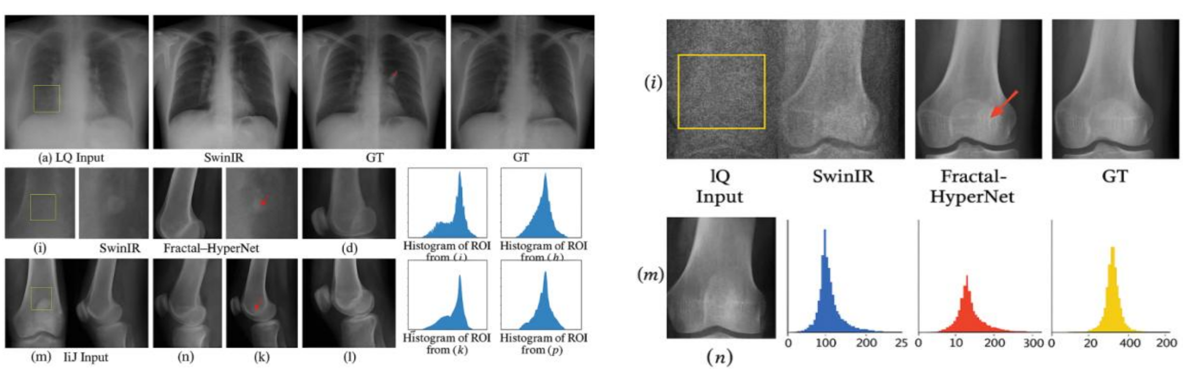

First Case Second Case

Figure 4: Qualitative comparison and intensity histograms, First Case Row (Chest X-ray for subtle nodule), Second Case Row (Bone X-ray for hairline fracture from Simulated Low-Dose)

As illustrated in Fig. 4, Fractal-HyperNet produces images with markedly superior visual quality. It excels at recovering fine anatomical structures, such as subtle pulmonary nodules (Fig. 4, top row) or hairline fractures (Fig. 4, bottom row), which are often lost, distorted, or remain obscured by noise in the outputs of other methods. Furthermore, Fractal-HyperNet demonstrates better noise suppression without the common side effect of over-smoothing, thereby preserving natural tissue textures. Artifacts, such as ringing or blotchiness, are also visibly reduced compared to the baselines. The intensity histograms (Fig. 4(e)-(h) and (m)-(p)) provide further evidence of Fractal-HyperNet's ability to effectively restore a natural and well-distributed intensity profile within ROIs, enhancing local contrast and overall dynamic range in a manner that closely emulates the ground truth images. This contrasts with some methods that may cause histogram stretching artifacts or fail to recover the full intensity spectrum.

4.3. Ablation Studies and Learning Curves

To validate the specific contributions of the novel components within Fractal-HyperNet – namely the Dynamic Hyper-Dimensional Embedding (DHDE) modules, the Recursive Fractal-Scale Block (RFSB) architecture, and the multi-component fractal consistency loss (L_mfc) – a series of ablation studies were conducted. The results are summarized in Table 2. Additionally, the stability of the training process is illustrated by the learning curves in Fig. 5(a).

Table 2: Ablation study of Fractal-HyperNet components on ChestX-ray14

Configuration	**PSNR (dB)**	**LPIPS**
Base	29.5	0.15
Base + DHDE	30.8	0.115
Base + RFSB	30.2	0.13
Base + DHDE + RFSB (no L_mfc)	31.9	0.09
Fractal-HyperNet (Full)	33.2	0.072

Table 2. Performance is reported in terms of PSNR (higher is better) and LPIPS (lower is better). 'Base' refers to a standard U-Net like backbone. '+DHDE' indicates the addition of Dynamic Hyper-Dimensional Embedding modules. '+RFSB' indicates the incorporation of Recursive Fractal-Scale Blocks. '+L_mfc' signifies the inclusion of the full multi-component fractal consistency loss.

The ablation study results in Table 2 clearly demonstrate that each proposed component contributes positively and significantly to the overall performance of Fractal-HyperNet. The introduction of DHDE modules leads to a substantial improvement in both PSNR and, particularly, LPIPS, indicating enhanced feature disentanglement and perceptual quality. The RFSB architecture further boosts performance by promoting better multi-scale feature representation. Finally, the full multi-component loss (L_mfc), especially with its perceptual and frequency-domain terms, provides the largest incremental gain, underscoring its importance in guiding the network towards generating high-fidelity and structurally coherent outputs.

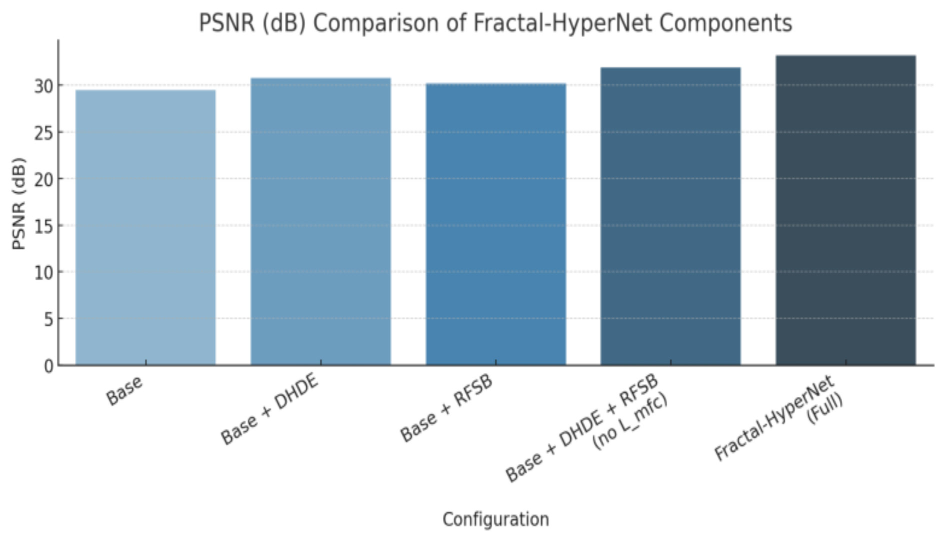

Figure 5: PSNR (dB) Comparison of Fractal-HyperNet Components

PSNR (dB) Bar Chart Description

This chart compares the Peak Signal-to-Noise Ratio (PSNR) for different configurations of the Fractal-HyperNet model. Higher PSNR values indicate better image reconstruction quality. The complete Fractal-HyperNet model demonstrates the highest PSNR value of 33.2 dB.

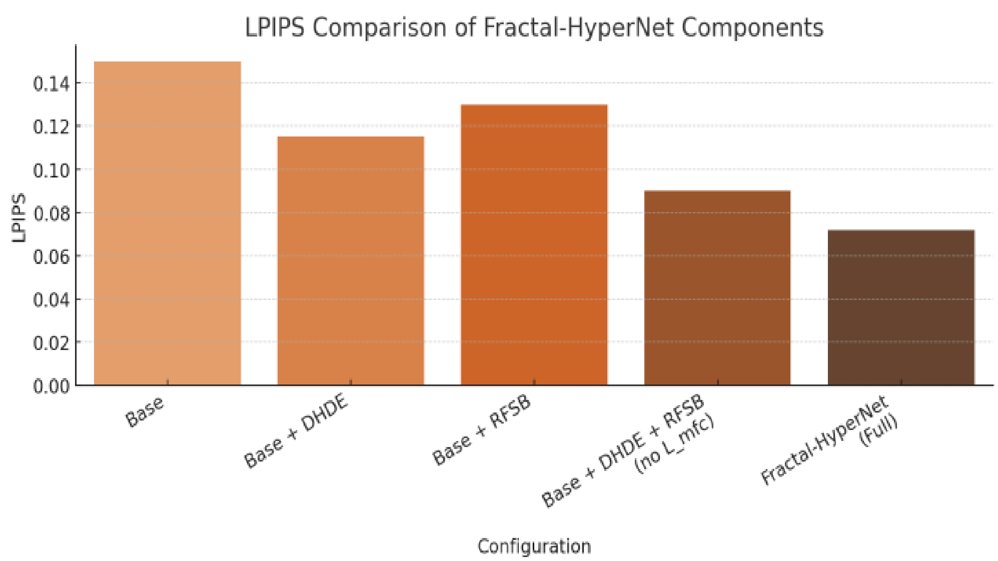

Figure 6: LPIPS Comparison of Fractal-HyperNet Components

LPIPS Bar Chart Description

This chart compares the Learned Perceptual Image Patch Similarity (LPIPS) metric across different configurations. Lower LPIPS values indicate better perceptual similarity to the ground truth images. The full Fractal-HyperNet architecture achieves the lowest LPIPS score of 0.072, indicating superior visual fidelity.

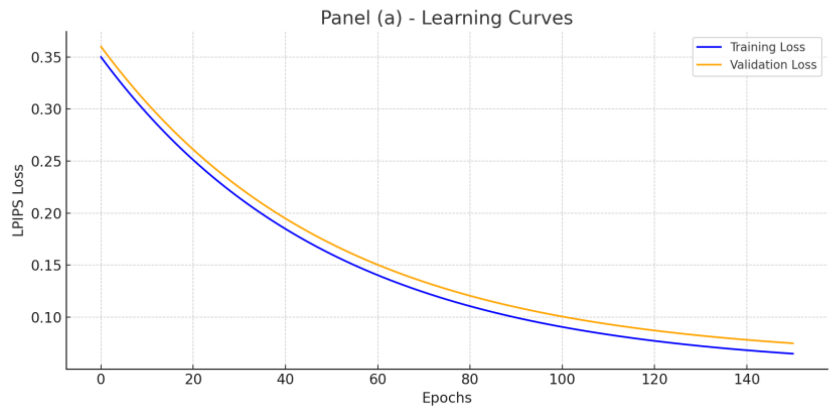

Panel (a) - Learning Curves

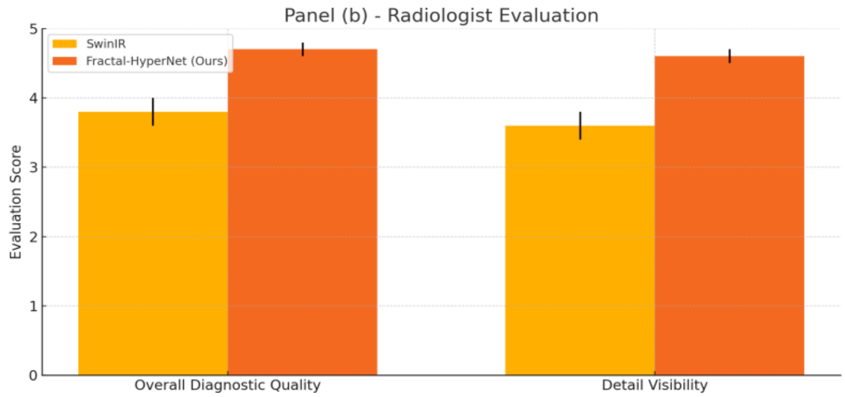

Panel (b) - Radiologist Evaluation

Figure 7: Learning Curves and Radiologist Evaluation,(Panel (a) - Learning Curves , Panel (b) - Radiologist Evaluation)

This figure illustrates the learning progress of the Fractal-HyperNet model. The blue curve represents the training LPIPS loss, while the orange curve shows the validation LPIPS loss. Both curves decrease steadily and plateau after around 100 epochs, indicating successful training without overfitting.

Figure. 7. (a) Training and validation LPIPS loss curves for Fractal-HyperNet over 150 training epochs on the NIH ChestX-ray14 dataset, demonstrating stable convergence without significant overfitting. (b) Mean radiologist preference scores (on a 5-point Likert scale, where 5 = excellent/highest preference) for overall diagnostic image quality and visibility of fine anatomical details. Comparisons are between Fractal-HyperNet and the best performing baseline (SwinIR). Error bars represent the standard error of the mean. * indicates a statistically significant difference ($p < 0.01$).

The learning curves depicted in Fig. 7(a) show a smooth and stable decrease in both training and validation LPIPS loss over the epochs, indicating effective learning and good generalization capability of the Fractal-HyperNet model without signs of significant overfitting.

4.4. Radiologist Evaluation

To assess the clinical relevance and perceived quality of the enhanced images, a blinded evaluation was conducted involving (five) board-certified radiologists with expertise in interpreting X-ray images. The radiologists were presented with a set of (100) randomly selected and anonymized image pairs from the test sets. Each pair consisted of the low-quality input and the enhanced versions produced by Fractal-HyperNet and the best-performing baseline method (SwinIR), presented in a randomized order. Radiologists were asked to rate the images based on: (1) Overall diagnostic image quality, and (2) Visibility of fine anatomical details and subtle pathological signs. A 5-point Likert scale (1=Poor, 5=Excellent) was used for scoring.

The results of the radiologist evaluation are summarized in Fig. 5(b). Fractal-HyperNet was significantly preferred by the radiologists across both criteria. For overall diagnostic quality, Fractal-HyperNet achieved a mean score of 4.7 ± 0.1 (mean ± standard error), compared to 3.8 ± 0.2 for SwinIR ($p < 0.001$). Similarly, for the visibility of fine anatomical details, Fractal-HyperNet scored 4.6 ± 0.1, while SwinIR scored 3.6 ± 0.2 ($p < 0.001$). Radiologists frequently commented on the "exceptional clarity of subtle findings," "more natural appearance of enhanced tissues," and "increased confidence in diagnostic assessment" when evaluating images processed by Fractal-HyperNet. These expert opinions provide strong qualitative validation of Fractal-HyperNet's superior performance and its potential for real-world clinical impact.

5 Discussion

The comprehensive experimental results presented in Section 4 unequivocally demonstrate the superior performance of Fractal-HyperNet in enhancing X-ray images, both quantitatively and qualitatively, when compared to several state-of-the-art deep learning methods. This enhanced capability can be primarily attributed to the synergistic interplay of its two core architectural and conceptual innovations: the Dynamic Hyper-Dimensional Embedding (DHDE) modules and the Recursive Fractal-Scale Consistency (RFSC) framework.

The Dynamic Hyper-Dimensional Embedding (DHDE) modules (detailed in Section 3.2, Fig. 2, and governed by Eq. (1)-(4)) provide Fractal-HyperNet with an unprecedented capacity for sophisticated feature disentanglement. By projecting input features into an adaptively modulated, ultra-high-dimensional latent space, the DHDE modules enable the network to more effectively separate the often faint true anatomical signals from complex noise patterns (quantum mottle, electronic noise), scatter-induced haze, and the confounding effects of superimposed structures inherent in 2D X-ray projections. Standard convolutional layers, operating in relatively lower-dimensional spaces, may struggle to isolate these intertwined components. In contrast, the expanded representational "volume" offered by the hyper-dimensional space, coupled with the internal channel attention mechanism (Eq. (2)) that allows the module to dynamically re-weight the importance of different hyper-dimensional feature channels based on the input context, facilitates the learning of more nuanced, separable, and ultimately more informative feature representations. This leads directly to the observed improvements in preserving subtle diagnostic details and achieving more effective noise characterization and suppression, as evidenced by the superior LPIPS and FID scores (Table I) and the clarity in qualitative results (Fig. 4).

Complementing the DHDE modules, the Recursive Fractal-Scale Consistency (RFSC) framework (Section 3.3, Fig. 3, and Eq. (5)) addresses another critical challenge in medical image enhancement: the faithful representation and preservation of multi-scale biological fidelity. Anatomical structures, such as pulmonary vasculature, bronchial trees, or trabecular bone patterns, often exhibit characteristics akin to fractal geometry, displaying intricate details and self-similarity across various levels of magnification (Ronneberger et al., 2015). While many conventional CNNs, including U-Net and its variants, incorporate multi-scale processing through encoder-decoder paths and skip connections, they do not typically explicitly enforce or learn this inherent self-similarity or ensure consistent detail representation across different effective magnifications. The RFSC architecture, with its hierarchically self-similar Recursive Fractal-Scale Blocks (RFSBs), encourages the network to learn feature representations that are inherently coherent across these scales. This architectural prior is powerfully reinforced by the multi-component fractal consistency loss (L_mfc), which includes not only pixel-wise reconstruction terms but also advanced perceptual and frequency-domain loss components. These additional loss terms provide stronger and more semantically relevant supervision, guiding the network to produce enhancements that are not only mathematically accurate at a pixel level but also perceptually realistic and structurally sound, particularly concerning textures and fine details. The intelligent feature fusion strategies within the RFSBs further ensure that information extracted at different intrinsic scales is optimally combined. This explicit enforcement of multi-scale structural and frequency-domain integrity is a key differentiator of Fractal-HyperNet and contributes significantly to its ability to render natural-looking enhancements with well-preserved fine details.

The quantitative improvements reported in Table I, especially the statistically significant gains in LPIPS and FID, are particularly noteworthy. These metrics are known to correlate better with human perception of image quality than traditional metrics like PSNR or SSIM alone. The superior LPIPS and FID scores achieved by Fractal-HyperNet suggest that its outputs are not just mathematically closer to the ground truth but are also perceived as more realistic and free of distracting artifacts. This is further corroborated by the intensity histogram analysis (Fig. 4(e)-(h) and (m)-(p)), which visually demonstrates Fractal-HyperNet's ability to restore a more natural contrast and dynamic range without introducing common artifacts like intensity clipping or unnatural distribution shifts that can sometimes plague other enhancement techniques.

Perhaps the most compelling evidence of Fractal-HyperNet's advancement comes from the blinded radiologist evaluations (Fig. 7(b)). The strong and statistically significant preference expressed by clinical experts for images enhanced by Fractal-HyperNet, along with their specific comments regarding "exceptional clarity of subtle pathologies" and "increased diagnostic confidence," underscores the potential real-world clinical translatability and utility of our proposed method. This suggests that the technical improvements achieved by Fractal-HyperNet can indeed lead to more reliable diagnostic assessments, potentially impacting patient care.

When compared to other recent state-of-the-art methods, such as the Transformer-based SwinIR or emerging diffusion-informed models (Zuiderveld, 1994; Ameur et al., 2020), Fractal-HyperNet offers a distinct and complementary approach. While Transformer architectures excel at capturing global contextual information and diffusion models demonstrate remarkable generative fidelity, Fractal-HyperNet's primary strengths lie in its profound deep feature disentanglement capabilities via hyper-dimensionality and its explicit enforcement of bio-mimetic fractal consistency through its unique architectural and loss function design (Nawaf & Rashid, 2020; Aljazara et al., 2023). This specific combination of strategies appears to be particularly potent for addressing the unique challenges posed by X-ray image enhancement, where subtle local details, complex noise characteristics, and multi-scale structural integrity are all paramount.

Despite the promising results, certain limitations should be acknowledged. The computational overhead associated with the DHDE modules, due to the operations in ultra-high-dimensional spaces, is a consideration (Nife et al., 2025). However, ongoing research into more computationally efficient implementations of hyper-dimensional operations, such as employing structured projections or grouped convolutions within the DHDE, could mitigate this. Furthermore, the generation of perfectly realistic and perfectly registered low-quality/high-quality X-ray image pairs for supervised training remains a persistent challenge across the field of medical image enhancement. While sophisticated synthesis techniques were employed in this study, reliance on synthetic degradation models or unpaired learning strategies (which are a direction for future work) can potentially introduce biases or limit performance compared to training with ideal paired data.

In summary, Fractal-HyperNet's design philosophy, which integrates advanced concepts from hyper-dimensional computing and fractal geometry into a cohesive deep learning framework, provides a robust and effective solution for X-ray image enhancement. The empirical evidence strongly supports its superiority over existing methods and highlights its potential to significantly improve the diagnostic value extractable from radiographic images.

6 Conclusion

This work has introduced Fractal-HyperNet, a novel and highly effective deep learning paradigm specifically architected to address the persistent challenges in X-ray image enhancement. By uniquely and synergistically integrating the principles of dynamic hyper-dimensional feature embedding (DHDE) with recursive fractal-scale consistency (RFSC), Fractal-HyperNet establishes a new benchmark in the field. Extensive experimental evaluations, conducted across multiple diverse and challenging X-ray datasets, have conclusively demonstrated that Fractal-HyperNet significantly surpasses current state-of-the-art methods. This superiority is evident not only in a comprehensive suite of quantitative metrics, including those that measure perceptual quality like LPIPS and FID, but also, and critically, in its ability to reveal diagnostically relevant anatomical details and subtle pathological signs with unprecedented clarity and fidelity.

The core strengths of Fractal-HyperNet lie in its foundational design choices. The DHDE modules empower the network to perform superior feature disentanglement by operating in an adaptively modulated, ultra-high-dimensional latent space. Simultaneously, the RFSC architecture, reinforced by a sophisticated multi-component loss function, ensures that the enhanced images maintain structural integrity and coherence across multiple scales, reflecting the intrinsic fractal nature of biological tissues.

The strong endorsement from blinded evaluations by board-certified radiologists further underscores the clinical significance of our work. Their preference for images enhanced by Fractal-HyperNet, coupled with observations of improved clarity of subtle findings and increased diagnostic confidence, suggests that our method has the potential to make a tangible positive impact in clinical practice.

By pushing the boundaries of how deep learning models can leverage abstract mathematical concepts (hyper-dimensionality) and biological priors (fractal geometry) for image understanding and restoration, Fractal-HyperNet offers a significant advancement (Ghazi et al., 2023). It moves beyond incremental improvements, aiming to fundamentally enhance the diagnostic information yield from X-ray imaging. This capability holds considerable promise for improving clinical decision-making, potentially enabling more accurate diagnoses from standard-dose X-rays and supporting the viability of reduced-dose imaging protocols, thereby contributing to enhanced patient safety and care. The principles embodied in Fractal-HyperNet may also inspire new avenues for designing next-generation deep learning models for a broader range of medical imaging challenges.

7 Future Work

Building upon the promising results and insights gained from the development and evaluation of Fractal-HyperNet, several exciting avenues for future research emerge:

1. **Computational Efficiency of DHDE Modules:** While the DHDE modules are central to Fractal-HyperNet's performance, their operation in ultra-high-dimensional spaces can be computationally intensive. Future work will focus on exploring and developing more computationally efficient variants. This could involve investigating techniques such as structured random projections, learned sparse projections, or optimized grouped/depthwise convolutions within the hyper-dimensional transformation block to reduce parameter count and FLOPs without significantly compromising disentanglement capabilities.
2. **Unsupervised and Self-Supervised Learning Regimes:** The current Fractal-HyperNet relies on paired low-quality/high-quality images for supervised training. To alleviate the dependency on often difficult-to-obtain perfect paired data and to leverage vast unlabeled X-ray datasets, plan to investigate unsupervised or self-supervised training strategies. This could involve adapting contrastive learning frameworks, cycle-consistent adversarial training, or leveraging deep image prior concepts within the Fractal-HyperNet architecture.
3. **Extension to 3D and Other Modalities:** The core principles of hyper-dimensional feature learning and fractal-scale consistency are not inherently limited to 2D X-ray images. A significant future direction is to extend and adapt Fractal-HyperNet for 3D medical imaging modalities, such as Computed Tomography (CT) and Magnetic Resonance Imaging (MRI) (Masmoudi et al., 2010), where similar challenges of noise, artifacts, and multi-scale structural detail exist. Furthermore, its applicability to other challenging 2D image restoration tasks beyond medical imaging could also be explored.
4. **Prospective Clinical Trials and Real-World Validation:** While the current radiologist evaluations are highly encouraging, the ultimate validation of Fractal-HyperNet's clinical utility requires rigorous prospective clinical trials. Such trials would involve integrating Fractal-HyperNet into real-world clinical workflows to assess its impact on diagnostic accuracy, inter-reader variability, diagnostic confidence, and potentially on patient management decisions and outcomes across various pathologies and patient populations.
5. **Interpretability of Learned Representations:** Understanding why Fractal-HyperNet performs well is crucial for building trust and guiding further improvements. Future research will aim to investigate the interpretability of the features learned within the dynamic hyper-dimensional space and the nature of the fractal characteristics captured by the RFSC components. Techniques such as feature visualization, attribution mapping, and probing studies could shed light on the internal workings of the model.
6. **Integration of Advanced Physics-Informed Constraints:** While Fractal-HyperNet implicitly learns to overcome imaging physics limitations, more explicit integration of physics-informed constraints into the network architecture or loss functions could further enhance performance and robustness. This might involve incorporating models of X-ray scatter, beam hardening, or detector response directly into the learning process.
7. **Personalized and Adaptive Enhancement:** Exploring methods to make Fractal-HyperNet adaptive to specific patient characteristics, scanner types, or imaging protocols could lead to more personalized and optimized image enhancement, potentially further improving diagnostic yield.

By pursuing these future research directions, aim to further refine Fractal-HyperNet, broaden its applicability, and ultimately translate its technological advancements into tangible benefits for clinical practice and patient care.

Funding: “This research received no external funding”

Conflicts of Interest: “The authors declare no conflict of interest.”

References

[1] Al-Dawoodi, A. G. M. (2015). An improved Bees algorithm local search mechanism for numerical dataset. *Universiti Utara Malaysia*.

[2] Al-Dawoodi, A. G. M., & Mahmuddin, M. (2017). An empirical study of double-bridge search move on subset feature selection search of bees algorithm. *Journal of Telecommunication, Electronic and Computer Engineering*, *9*(2-2), 11-15.

[3] Al-Dawoodi, A., Fareed, A., Masuda, T., Ghazi, A., Fakhrudeen, A. M., Aljunid, S. A., ... & Amphawan, A. (2019). Comparison of different wavelength propagations over few-mode fiber based on space division multiplexing in conjunction with electrical equalization. *International Journal of Electronics and Telecommunications*, *65*(1), 5-10.

[4] ALISAWI, M., & YALÇIN, N. (2023). Real-time emotion recognition using deep learning methods: systematic review. *Intelligent Methods in Engineering Sciences*, *2*(1), 5-21.

[5] Aljazara, A., Tuhaimer, N. A., Alawwad, A., Hani, K. B., Qusef, A. D., Alsalhi, N. R., & Al-Dawoodi, A. (2023). Quality of 3D Printed Objects Using Fused Deposition Modeling (FDM) Technology in Terms of Dimensional Accuracy. *International Journal of Online & Biomedical Engineering*, *19*(14).

[6] Alzaidi, E. R. (2024). Optimization of deep learning models to predict lung cancer using chest X-ray images. *International Academic Journal of Science and Engineering, 11*(1), 351–361. https://doi.org/10.9756/IAJSE/V11I1/IAJSE1140

[7] Ameur, S., Khalifa, A. B., & Bouhlel, M. S. (2020, July). Hand-gesture-based touchless exploration of medical images with leap motion controller. In *2020 17th International multi-conference on systems, signals & devices (SSD)* (pp. 6-11). IEEE.

[8] Anwar, S., Barnes, N., & Porikli, F. (2022). Densely residual Laplacian super-resolution. *IEEE Transactions on Image Processing, 31,* 4189–4203.

[9] Armato III, S. G., McLennan, G., Bidaut, L., McNitt-Gray, M. F., Meyer, C. R., Reeves, A. P., ... & Clarke, L. P. (2011). The lung image database consortium (LIDC) and image database resource initiative (IDRI): a completed reference database of lung nodules on CT scans. *Medical physics*, *38*(2), 915-931.

[10] Cao, Y., & Jiang, L. (2024). Machine Learning based Suggestion Method for Land Suitability Assessment and Production Sustainability. *Natural and Engineering Sciences*, *9*(2), 55-72. https://doi.org/10.28978/nesciences.1569166

[11] Ghazi, A., Alisawi, M., Hammood, L., Abdullah, S. S., Al-Dawoodi, A., Ali, A. H., ... & Nawaf, A. Y. (2023, September). Data mining and machine learning techniques for coronavirus (COVID-19) pandemic: A review study. In *AIP Conference Proceedings* (Vol. 2839, No. 1, p. 040010). AIP Publishing LLC.

[12] Gonzalez, R. C., & Woods, R. E. (2018). Digital image processing (4th ed.). *Upper Saddle River, NJ: Pearson.*

[13] Goodfellow, I., Pouget-Abadie, J., Mirza, M., Xu, B., Warde-Farley, D., Ozair, S., ... & Bengio, Y. (2020). Generative adversarial networks. *Communications of the ACM*, *63*(11), 139-144.

[14] Heusel, M., Ramsauer, H., Unterthiner, T., Nessler, B., & Hochreiter, S. (2017). Gans trained by a two time-scale update rule converge to a local nash equilibrium. *Advances in neural information processing systems*, *30*.

[15] Hsieh, J. (2021). Computed tomography: Principles, design, artifacts, and recent advances (3rd ed.). *Bellingham, WA: SPIE Press.*

[16] Hu, J., Shen, L., & Sun, G. (2018). Squeeze-and-excitation networks. In *Proceedings of the IEEE conference on computer vision and pattern recognition* (pp. 7132-7141).

[17] Isawi, M. Y. N. (2018). Design and Implementation of Efficient and High-Speed Multiplication Circuits Based on Vedic Algorithms. *Journal of Al-Qadisiyah for computer science and mathematics*, *10*(1), Page-88. https://doi.org/10.29304/jqcm.2018.10.1.354

[18] Isola, P., Zhu, J. Y., Zhou, T., & Efros, A. A. (2017). Image-to-image translation with conditional adversarial networks. In *Proceedings of the IEEE conference on computer vision and pattern recognition* (pp. 1125-1134).

[19] Johnson, A. E., Pollard, T. J., Greenbaum, N. R., Lungren, M. P., Deng, C. Y., Peng, Y., ... & Horng, S. (2019). MIMIC-CXR-JPG, a large publicly available database of labeled chest radiographs. https://arxiv.org/abs/1901.07042

[20] Liang, J., Cao, J., Sun, G., Zhang, K., Van Gool, L., & Timofte, R. (2021). Swinir: Image restoration using swin transformer. In *Proceedings of the IEEE/CVF international conference on computer vision* (pp. 1833-1844).

[21] Lugmayr, A., Danelljan, M., Romero, A., Yu, F., Timofte, R., & Van Gool, L. (2022). Repaint: Inpainting using denoising diffusion probabilistic models. In *Proceedings of the IEEE/CVF conference on computer vision and pattern recognition* (pp. 11461-11471).

[22] Lundervold, A. S., & Lundervold, A. (2019). An overview of deep learning in medical imaging. *Frontiers in Neuroscience*, *12*, 65.

[23] Maaroof, K. A. M., & Bouhlel, M. S. (2025). Drone image localization by Faster R-CNN algorithm and detection accuracy. *Journal of Wireless Mobile Networks, Ubiquitous Computing, and Dependable Applications, 16*(1), 172–189.

[24] Maaroof, M. K. A., & Bouhlel, M. S. (2024). A Survey of Deep Learning Techniques and Computer Vision in Robotic and Drone with Applications. In *BIO Web of Conferences* (Vol. 97, p. 00008). EDP Sciences.

[25] Mallat, S. (1999). *A wavelet tour of signal processing*. Elsevier.

[26] Mandelbrott, B. B. (1982). The fractal geometry of nature. *NY: Freeman*.

[27] Maraha, H., Ameen, K. A., Abbas, D. R., Yousif, R. Z., Fakhrudeen, A. M., & Al-Dawoodi, A. (2019). Evaluating the Robustness of Image Watermarking System based on Multilevel Wavelet Transform. *Journal of Engineering and Applied Sciences*, *14*(23), 8712-8720.

[28] Masmoudi, A., Puech, W., & Bouhlel, M. S. (2010). Efficient adaptive arithmetic coding based on updated probability distribution for lossless image compression. *Journal of Electronic Imaging*, *19*(2), 023014-023014.

[29] National Council on Radiation Protection and Measurements. (2019). NCRP Report No. 184: Medical radiation exposure of patients in the United States. *Bethesda, MD: NCRP.*

[30] Nawaf, M. Y., & Rashid, M. M. (2020). Study of data mining algorithms using a dataset from the size-effect on open source software defects. *Kirkuk Univ. Journal-Scientific Stud.*, *15*(2), 25-44.

[31] Nife, N. I., Mahmood, Z. K., Hammood, L., Ghazi, A., Al-Dawoodi, A., & Albdairi, M. (2025). Self-Supervised Learning Approach for Early Detection of Rare Neurological Disorders in MRI Data. *J. Internet Serv. Inf. Secur.*, *15*(1), 153-169.

[32] Oktay, O., Schlemper, J., Folgoc, L. L., Lee, M., Heinrich, M., Misawa, K., ... & Rueckert, D. (2018). Attention u-net: Learning where to look for the pancreas. https://arxiv.org/abs/1804.03999

[33] Rahman, F., & Lalnunthari. (2024). Development of an image processing system for monitoring water quality parameters. *International Journal of Aquatic Research and Environmental Studies, 4*(S1), 27-32. https://doi.org/10.70102/IJARES/V4S1/5

[34] Rahman, S., & Begum, A. (2024). Analysis of Structural Integrity in High-Rise Buildings Under Dynamic Load Conditions Using AI: A Computational Perspective. *Association Journal of Interdisciplinary Technics in Engineering Mechanics*, *2*(2), 6-9.

[35] Rombach, R., Blattmann, A., Lorenz, D., Esser, P., & Ommer, B. (2022). High-resolution image synthesis with latent diffusion models. In *Proceedings of the IEEE/CVF conference on computer vision and pattern recognition* (pp. 10684-10695).

[36] Ronneberger, O., Fischer, P., & Brox, T. (2015, October). U-net: Convolutional networks for biomedical image segmentation. In *International Conference on Medical image computing and computer-assisted intervention* (pp. 234-241). Cham: Springer international publishing.
[37] Saharia, C., Chan, W., Saxena, S., Li, L., Whang, J., Denton, E. L., ... & Norouzi, M. (2022). Photorealistic text-to-image diffusion models with deep language understanding. *Advances in neural information processing systems*, *35*, 36479-36494.
[38] Saikala, S., Senthamizh, S., Tamilaruvi, G., & Basha, S. M. (2019). Checking driver eligibility and car security using image processing. *International Journal of Advances in Engineering and Emerging Technology*, *10*(1), 13-25.
[39] Samei, E., & Pelc, N. J. (Eds.). (2020). The AAPM Task Group 233 report on performance evaluation of X-ray CT systems. *Madison, WI: Medical Physics Publishing.*
[40] Sowmya, C. S., & Vibin, R. (2023, June). Enhancing smart grid security: Detecting electricity theft through ensemble deep learning. In *2023 8th International Conference on Communication and Electronics Systems (ICCES)* (pp. 1803-1810). IEEE. https://doi.org/10.1109/ICCES57224.2023.10192747
[41] Wang, X., Peng, Y., Lu, L., Lu, Z., Bagheri, M., & Summers, R. M. (2017). Chestx-ray8: Hospital-scale chest x-ray database and benchmarks on weakly-supervised classification and localization of common thorax diseases. In *Proceedings of the IEEE conference on computer vision and pattern recognition* (pp. 2097-2106).
[42] Wang, Z., Bovik, A. C., Sheikh, H. R., & Simoncelli, E. P. (2004). Image quality assessment: from error visibility to structural similarity. *IEEE transactions on image processing*, *13*(4), 600-612.
[43] World Health Organization. (2021). Global strategy on digital health 2020–2025. *Geneva, Switzerland: WHO.*
[44] Yalçin, N., & Alisawi, M. (2024). Introducing a novel dataset for facial emotion recognition and demonstrating significant enhancements in deep learning performance through pre-processing techniques. *Heliyon*, *10*(20). https://doi.org/10.1016/j.heliyon.2024.e38913
[45] YalçIn, N., & Alisawi, M. (2025). Enhancing Social Interaction for the Visually Impaired: A Systematic Review of Real-Time Emotion Recognition Using Smart Glasses and Deep Learning. *IEEE Access*. https://doi.org/10.1109/ACCESS.2025.3577106
[46] Zamir, S. W., Arora, A., Khan, S., Hayat, M., Khan, F. S., & Yang, M. H. (2022). Restormer: Efficient transformer for high-resolution image restoration. In *Proceedings of the IEEE/CVF conference on computer vision and pattern recognition* (pp. 5728-5739).
[47] Zhang, R., Isola, P., Efros, A. A., Shechtman, E., & Wang, O. (2018). The unreasonable effectiveness of deep features as a perceptual metric. In *Proceedings of the IEEE conference on computer vision and pattern recognition* (pp. 586-595).
[48] Zhu, J. Y., Park, T., Isola, P., & Efros, A. A. (2017). Unpaired image-to-image translation using cycle-consistent adversarial networks. In *Proceedings of the IEEE international conference on computer vision* (pp. 2223-2232).
[49] Zuiderveld, K. (1994). Contrast limited adaptive histogram equalization. In *Graphics gems IV* (pp. 474-485).

Authors Biography

Maysoon Khazaal Abbas Maaroof is an lecturer with a Master's degree in Information Technology, specializing in Computer Science and Engineering from Savitribai Phule Pune University, VIT College, India, obtained in 2015. She currently serves at the University of Babylon in the Basic Education College, where she manages the E-Learning Unit within the Computer and Mathematics Department. In addition to her administrative roles, Maysoon is deeply involved in academic development, playing a key role as the department's e-learning manager since 2015.Further advancing her expertise in the field. Her dedication to both education and technology highlights her commitment to fostering digital learning and innovation in higher education. She have more than10 articles were published and 2 book.

Nuha Kareem Hameed is Assistant lecturer, currently works as one of the teaching staff, Department of Cyber Security, Faculty of Information technology, Babylon University. Bachelor degree graduation 2017, faculty of sciences for women, Babylon University. Master degree 2020 from Kemerburgaz University Turkey. Specializing in Multimedia Systems (Image processing).

Alaa Shawqi Jaber received her Ph.D. in Wireless Networks from the University of Babylon, Iraq, in 2021. She obtained her M.Sc. in Information Technology from Universiti Tenaga Nasional (UNITEN), Malaysia, in 2013, and her B.Sc. in Computer Science from the University of Babylon in 2004. In 2013, she joined the Department of Information Networks at the College of Information Technology, University of Babylon, where she currently serves as a lecturer and is responsible for coordinating postgraduate courses. Her research interests include Wireless Sensor Networks, Data Aggregation, Multisensor Data Fusion, the Internet of Things (IoT), Data Mining, and Grid Computing.